Temperature Tailored Molten Salts for Sustainable Energy Storage

Marco Bernagozzi, Angad Panesar*, Robert Morgan
Advanced Engineering Centre, School of Computing, Engineering and Mathematics, University of Brighton, United Kingdom
*Corresponding Author: A.S.Panesar@brighton.ac.uk

Abstract

The power generation sector is moving towards more renewable energy sources to reduce CO_2 emissions by employing technologies such as the concentrated solar power plants and the liquid air energy storage systems. This work was focused on the identification of new molten salt mixtures to act as both, the thermal energy store and the heat transfer fluid in such applications. Firstly, a selection process utilizing literature data and Aspen$^+$ property package led to the identification of 5 nitrate-based mixtures offering suitable trade-off between melting point temperatures and volumetric heat capacities. Secondly, new salt compositions with improved volumetric heat capacities were created from the starting-point commercial molten salt mixtures, and then, experimentally tested for evaluating the melting point. Finally, volumetric heat capacity maps were created for the different temperature regimes, indicating 3 new temperature tailored molten salt mixtures, which use the same pure constituents as that of CaLiNaK and Quaternary.

1. Introduction

Global warming has increased the focus of the power generation sector to reduce CO_2 emissions by utilizing lesser fossil fuels and greater renewable energy sources. The European Union has set a target for renewable energy to constitute 20% of the total energy produced by 2020 [1]. The very nature of renewable energy sources carries a series of intrinsic complexities in balancing the energy network, such as less flexibility, intermittent operation and geographical dependency. This makes it complex to combine the most prominent renewable energy sources (Wind, Hydro and Solar) with the power grid, as generation and consumption need to be constantly matched. Electric energy storage can partially mitigate these issues, allowing to store energy when the production exceeds demand and to discharge it to the power grid when needed [2]. Amongst the technologies for sustainable energy production, two are gaining increasing interest from the research community: Concentrated Solar Power (CSP) and Liquid Air Energy Storage (LAES).

CSP plants use solar collectors that reflects direct sun irradiation to a thermal receiver system, hence, increasing the solar radiation flux density. This allows for higher temperatures and higher conversion efficiencies from optical energy to thermal energy [3]. Typically, there are two main groups of CSPs: line focusing, which comprise of parabolic trough and linear Fresnel reflector, and point focusing, which can be central receiver type or parabolic dish type.

Parabolic trough is characterized by the use of parabolic shaped mirrors to focus sunlight onto an evacuated absorber tube receiver, while mirrors and tubes follow the daily sun movement. This typology is the most diffused as it provides the highest efficiency. Linear Fresnel systems use individual planar mirrors to focus sunlight on a downward-facing tube receiver. Typical operating temperatures of linear Fresnel plants are between 290-390 °C with peak and annual average conversion efficiencies of 14-20% and 13-15%, respectively [4]. Furthermore, they can reduce the costs with respect to parabolic trough.

Point focusing systems are typically based on two-axial mirrors, called heliostats, systems that allow for high concentration ratios and higher temperatures in the receiver, which can be either a solar tower or a dish system, when compared to linear Fresnel systems. The high operation temperatures between 290-565°C results in higher peak of 23-35% and annual conversion efficiencies of 14-18% [5].

During day time operation, surplus energy generated is stored in a Thermal Energy Storage (TES), which is used to heat the working fluid of the thermal cycle during discharging, increasing the overall system efficiency [6]. Moreover, a TES can increase the system reliability and reduce the energy cost for the customer. It was estimated that a TES used to store energy produced in excess during day operation could improve the capacity factor from 20-25% to 60-85% [7].

An additional interesting solution for sustainable energy production is the Liquid Air Energy Storage (LAES) which is gaining interest due to its advantages such as: large volumetric energy density, no geographical dependency, no pollution and long operative life [8]. LAES working principle is threefold: electrical energy is used to liquefy air via compression and refrigeration; cold liquefied air is stored in low pressure insulated tanks; when the grid requires additional power, liquid is drawn from the tank, heated and expanded in a turbine connected to a generator [9]. Currently, there is only one MW-scale LAES plant in operation. This is located near Manchester (UK) and managed by Highview Power Storage Ltd. The LAES system is distinct from the Compressed Air Energy Storage (CAES) system, where the thermal medium is compressed air [10].

Similar to CSP plants, LAES can employ a TES system, especially for the recovery of excess heat during the charging process (i.e. air liquefaction). It has been reported that, there is a 20-40% excess heat of compression, which currently is not being used effectively [11], and can therefore be recovered. This thermal energy can be used to heat up the air during the discharging process (i.e. evaporation), hence increasing the overall system efficiency.

The TES medium proposed in the present work is molten salts because of their appealing features such as [12]: low melting point, ultra-low vapour pressure, high volumetric heat capacity, no spontaneous detrimental exothermic reactions, insensibility to radiations and the fact that they can be liquid over a wide operative temperature range. Moreover, they present good stability at high temperatures [13]. When compared against conventional coolants, they allow lower heat exchanger costs, as they provide volumetric heat capacities 25% higher than pressurised water and five times higher than liquid sodium. Furthermore, they have been utilised as TES fluid in several CSP plants, including, USA (Solar Two), Spain (CESA I-PSA) and France (THEMIS) [14]. TES technology with molten salt can be either direct or indirect. In direct molten salt storage, the salt is used to directly heat the working fluid used for the energy conversion. In indirect molten salt storage, the salt is an intermediary as it heats a HTF, such as thermal oil, which will then heat the working fluid for the power generation [15]. Research recently is focusing on the development of lower melting point molten salts in order to reduce the usage of solutions such as heat tracing tapes, thermal insulation, and to reduce the risk of freezing inside the pipes [16]. This would reduce the initial capital investment as well as the running costs.

An interesting feature of such industrial applications is that, the molten salts are also being used as the Heat Transfer Fluid (HTF), thereby reducing the system complexity. In fact, molten salts have been used as coolants in the so-called Molten Salt Reactors (MSR), where a fluoride salt (FLiBe) is used as coolant. This offers several key benefits such as high degree of passive safety, atmospheric pressure operation, lower spent fuel per unit of energy, and high solubility of most fission products in molten salts [17].

This work is focused on the identification of new molten salt mixtures that offer low to medium melting temperatures and beneficial thermo-physical properties, in order to be used as both TES and HTF in CSP and LAES plants. Firstly, selection of low melting point molten salt mixtures using the published literature was conducted, resulting in the choice of 5 starting-point commercial salt mixtures for further investigation. Secondly, utilising the same constituents as the starting-point mixtures, several new salt compositions were evaluated in terms of volumetric heat capacity using the Aspen^{+} simulation platform employing an advanced simulation procedure. Subsequently, experimental investigations were conducted to identify the melting point of 13 new mixtures. Finally, three maps presenting melting temperature and volumetric heat capacity of the starting-point as well as the alternative mixtures, with particular focus on three different temperature ranges (< 100˚C, 100-150˚C, < 200˚C) were created, with the aim to provide a better guide in selecting the correct molten salt for a particular application.

2. Salt Mixture Selection and Hybrid Simulation Procedure

The aim of the present work was to investigate new molten salt mixtures to be used for both TES and HTF. For the first phase of down-selection, the melting temperature of < 200˚C was chosen, as it indicates the common range for CSP and LAES applications. Table I presents the starting-point salts and their melting point, as a result of the initial down-selection process performed following a comprehensive review of molten salts data. The nitrate and chloride salt families offered comparable average melting point temperatures (113 vs. 108˚C). Note that, solar salt is only included as a reference due to its use in CSP plants [18].

Table I. Starting-point commercial molten salts (nitrate and chloride families) with low melting point temperature.

Salt	Composition	T_m[°C]	Ref
HITEC	7NaNO3-40NaNO2-53KNO3 (7-40-53)	142	[12]
LiNaK	18NaNO3-52KNO3-30LiNO3 (18-52-30)	120	[19]
LiK	68KNO3-32LiNO3 (68-32)	133	[20]
Quaternary	14.2NaNO3-50.5KNO3-17.5LiNO3-17.8NaNO2 (14.2-50.5-17.5-17.8)	99	[21]
CaLiNaK	24.6LiNO3-13.6Ca(NO3)2-16.8NaNO2-15KNO2 (24.6-13.6-16.8-15)	72	[15]
NaCl-AlCl3	20NaCl-80AlCl3 (20-80)	108	[21]
KCl-AlCl3	22KCl-78AlCl3 (22-78)	128	[21]
KCl-AlCl3-NaCl	11KCl-78AlCl3-11NaCl (11-78-11)	89	[21]
Solar Salt	60NaNO3-40KNO3 (60-40)	222	[12]

In the second phase of down-selection, the critical thermo-physical property, i.e. the volumetric heat capacity, was considered. However, as highlighted by Nunes et al. [22], there is a noticeable fragmentation and ambiguity in the published data on salt properties, as diverging trends and incomparable temperature ranges have been

reported. Hence, a detailed literature review was conducted, and a database of the most relevant thermo-physical properties for all pure salts that make-up the starting-point mixtures reported in Table I was created.

2.1. Hybrid Simulation Procedure

To mitigate the challenges highlighted by Nunes et al. [22], a hybrid simulation procedure was developed. Firstly, the thermo-physical property database of pure salts were imposed in Aspen+. This allowed replication of the trends reported in the literature, regardless of their limited validity range. Secondly, in order to provide a continuous set of information over the interested temperature range (100°C to 400˚C), different equations reported in the literature were coupled, including suitable Aspen$^+$ property packages. Fig.1 reports two such hybrid procedure examples, for $NaNO_3$ and $NaNO_2$ respectively.

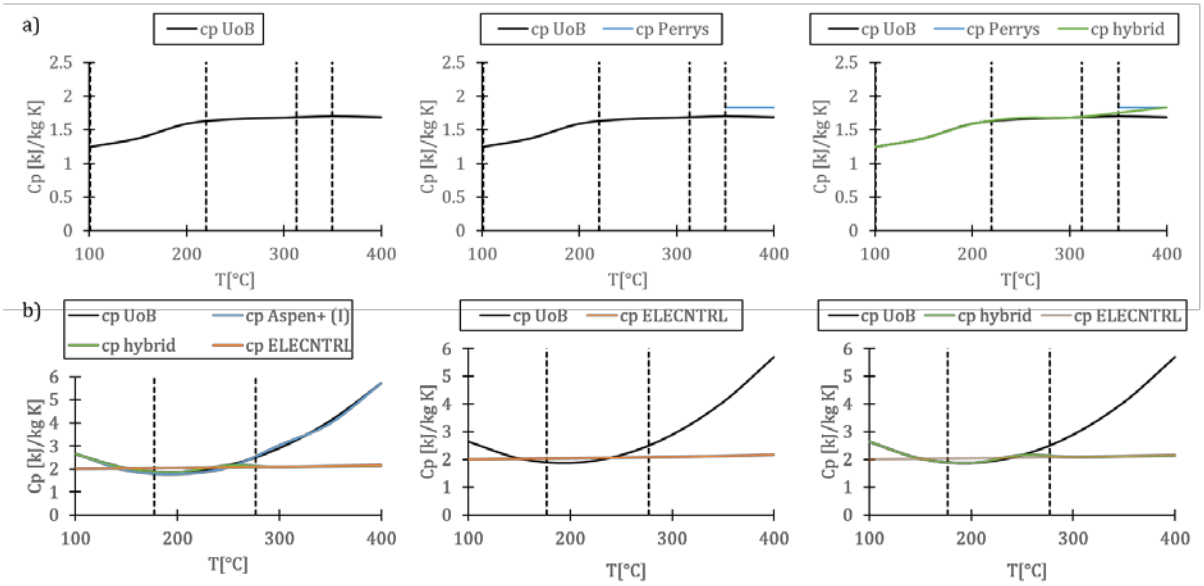

Fig.1. Hybrid simulation procedure applied to pure salts: a) $NaNO_3$ mass heat capacity and b) $NaNO_2$ mass heat capacity. UoB refers to the compiled database; Perrys refers to the Perry's Database; ELECNTRL refers to the suitable Aspen$^+$ Property Package; Hybrid refers to the advanced simulation procedure introduce herein.

In Fig.1a, different correlations reported in the literature are merged together. The black dashed lines represent the validity ranges of the two different equations. The solid black line (UoB) is the result of the compiled database utilising [23] and is suitable between 100-220°C and 313-350°C. Furthermore, the solid blue line (Perrys) is the result of Perry's handbook [24] and is suitable for > 350°C. By merging these two results, the solid green line (hybrid) is produced, exploiting findings published over the years.

In Fig.1b, a correlation reported the literature is merged together with the suitable Aspen+ Property Package. The solid black line (UoB) is the result of the compiled database utilising [25] and is suitable between 177-277°C. Furthermore, the solid orange line (ELECNTRL) is the result of the existing property package in Aspen$^+$ best matched to what is reported in the literature. By merging these two results, the solid green line (hybrid) is produced. This allowed improvements in the overall accuracy of the simulation, not only for pure salts, but also for mixtures, as detailed below.

The next step was to simulate and replicate the thermo-physical properties of the starting-point salt mixtures against the scarcely available data. Aspen$^+$ is an advanced software that allows, once given the correct properties of the pure constituents, to correctly estimate thermo-physical properties of the mixtures. Fig.2 illustrates the advantage of using the hybrid simulation procedure for mixture modelling. The solid black line (UoB) represents the literature data for the HITEC mixture. The solid blue line (x) represents the result if the pure salts from the compiled database are utilized for the mixture. Whereas, the solid green line (hybrid) represents the result if the hybrid approach outcome of pure salts are utilized for the mixture in Aspen$^+$. Hence, this advanced simulation procedure allowed reproduction of the key thermo-physical properties of mixtures with low errors of 0.4-13% over a wide temperature range.

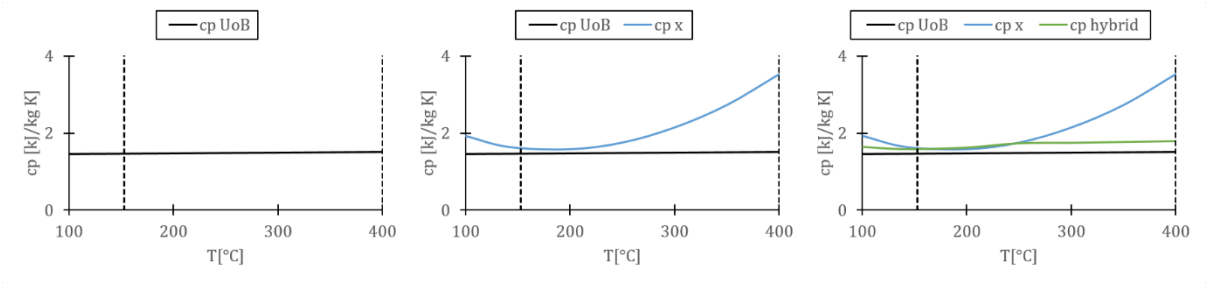

Fig.2. Hybrid simulation procedure applied to salt mixtures (e.g. HITEC). Black line refers to the literature data; Blue line refers to the mixture obtained using the compiled database of pure salts; Green line refers to the mixture obtained by using the hybrid approach outcome of pure salts in Aspen^{+}.

2.2. Volumetric Heat Capacity

The ability to accurately reproduce the thermo-physical properties of the starting-point commercial salt mixtures, gave high confidence in estimating the thermo-physical properties not yet published in literature, for both the remaining commercial salt mixtures as well as their alternative weight compositions. This allowed to proceed with the second phase of the down-selection process, which was the evaluation of the thermo-physical properties in the temperature range of 100-400°C. The most relevant of these properties being the volumetric heat capacity, defined in eq.1. As maximizing this quantity reduces the size of vessels and heat exchangers, hence, reducing the cost and complexity of the plant.

$$c_v = c_p \rho \qquad (1)$$

Fig.3 presents the variation in volumetric heat capacity for the starting-point commercial molten salt mixtures in the temperature range of application, obtained following the hybrid simulation procedure in Aspen^{+}. It is evident how the chloride-based salt mixtures provided lower values of volumetric heat capacities compared to the nitrate-based salt mixtures (1.7-2.2 vs. 2.8-3.1 MJ/m^{3}K). Hence, the chloride-based salt mixtures were disregarded from further consideration in the present work.

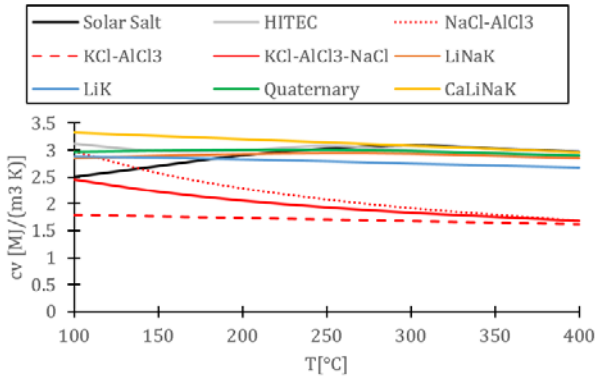

Fig.3. Volumetric heat capacity variation of the starting-point commercial molten salt mixtures.

A good compatibility of the chosen salts with the plant materials is vital [17]. Hence, information was compiled from several manufactures databanks (such as Cole Parmer, eFunda, Allorings, Trelleborg, Graco and Colder Products) concerning the compatibility with common materials of the pure salts which are constituents of the selected mixtures. Table II shows the results of this survey, ranking the compatibility on a scale from 1 (highly suitably) to 4 (zero suitability). This scale captures the swelling percentage in the case of the elastomer/plastic and the amount of µm lost over a year for metals. More importantly, the nitrate-based pure salts offered a wide compatibility.

Table II. Compatibility of the pure salts which are constituents of the selected mixtures with common metal and plastics; Legend: 1 = Good; 2 = Fair; 3 = Poor; 4 = Bad. The below data refer to a 48hr exposure time at 21-22°C room temperature.

Material	$NaNO_3$	KNO_3	$NaNO_2$	$Ca(NO_3)_2$	$LiNO_3$
ABS plastic		2		1	
Aluminum	2	2	1	2	
Carbon graphite	3	1		1	
Carbon Steel	2	2		2	
Cast iron	2	1	1	2	

Ceramic Al203	1	2		1	
Copper	4	1			
Ethylene-Propylene	1	1	1	1	1
Polycarbonate		1		1	
Polypropylene	1	1	1	1	
Polyurethane	2	1	4	4	
PTFE	1	1	1	1	
Silicone	4	1	4	2	2
SS 304	2	2	1	3	
SS 316	2	2		2	
Teflon	1	1	1	1	
Titanium	1	1		2	

The down-selection process summarised above resulted in the choice of HITEC, LiNaK, LiK, Quaternary and CaLiNaK as the 5 starting-point commercial salt mixtures for continued investigation. Table III details the compositions of these molten salt mixtures expressed in mass fraction.

Table III. Chosen 5 starting-point molten salt mixture compositions expressed in mass fractions.

Molten Salt Name	Composition
HITEC	7NaNO3-40NaNO2-53KNO3
LiNaK	28NaNO3-52KNO3-20LiNO3
LiK	68KNO3-32LiNO3
Quaternary	14.2NaNO3-50.5KNO3-17.5LiNO3-17.8NaNO2
CaLiNaK	24.6LiNO3-13.6Ca(NO3)2-16.8NaNO2-15KNO2

3. Experimental Melting Point

New molten salt mixtures were simulated in Aspen^{+} by varying the mass fractions of the pure salt constituents in the 5 chosen starting-point commercial salts. For the parametric analysis, the variable of interest was the volumetric heat capacity, as it was identified as an important parameter during the down-selection process. Two classifications of mixtures were considered: similar composition to starting-point salt mixtures, and noticeably different composition to starting-point salt mixtures but offering significantly higher volumetric heat capacity. As a result, a total of 13 out of 70 simulated alternative new molten salt mixtures were considered for experimental identification of melting point temperature. Mass fraction variations that provided volumetric heat capacity lower than its starting-point salt was disregarded from consideration.

The experimental method, depicted in Fig.4 included the preparation of alternative salt mixture concentrations using the pure salts (KNO_3, $NaNO_3$, $NaNO_2$, $LiNO_3$, $CaNO3{\bullet}4H_2O$, 99% purity, Merck®). To ensure fine homogenous mixture, mass fractions were prepared using Kern® weighing scale (resolution 0.1 mg) and mixed using Camlab® vortex mixer. To limit sensibility errors relating to small weight fractions of pure salts, the minimum quantity prepared for salt mixtures was 5 grams.

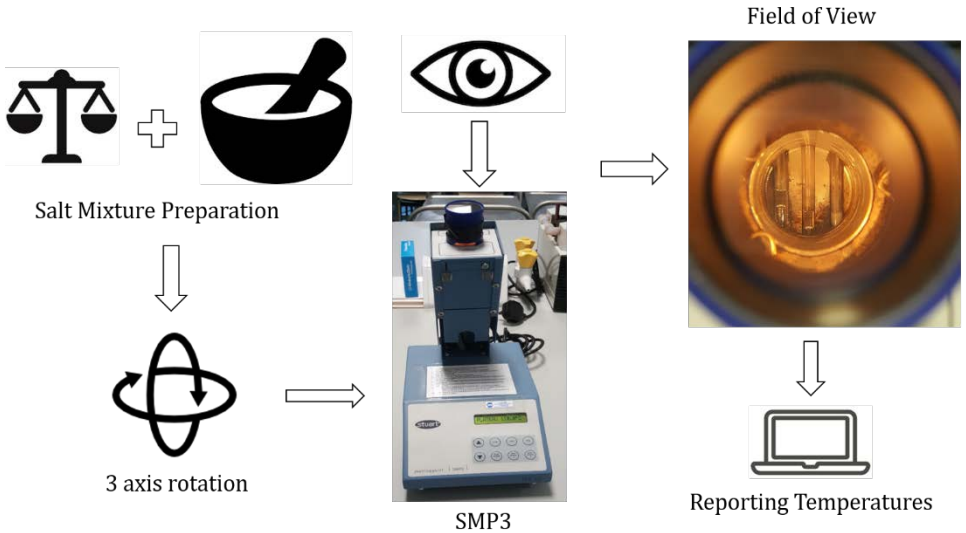

Fig.4. Concentration preparation and homogenous mixing followed by observation and measurement of melting point.

For measuring the melting point, the Stuart® SMP3 was used. It was observed that, due to the small diameter of the capillary tubes, the preparation of a fine mixture was important, as well as ensuring a proper mixing.

Otherwise, clusters of single salt were observed in the tube, resulting in an incomplete melting of the mixture. In order to ensure the correct implementation of the experimental procedure, thermal cycling was performed on the samples, resulting in the same melting temperature in majority of the test cases. In those test cases where the melting point had varied, the result was disregarded.

This allowed the simultaneous testing of three capillary samples (Stuart® OD/ID 1.9mm/1.3mm) with a fine control (±0.1°C/min) of the heating ramp rate. During testing of each mixture, a fast 5˚C/min ramp rate was applied until the plateau temperature was reached, which was set at 30˚C lower than the melting temperature of the starting-point commercial salt mixture. Once the plateau temperature was reached, a slower 1˚C/min ramp rate was applied. In order to gain enough precision, for each salt mixture, three tests were conducted and the mean values are reported. The melting temperature was calculated using the standard approach [26]:

$$T_m = \frac{T_{m,1} + T_{m,2}}{2} \quad (2)$$

where $T_{m,1}$ is the temperature at which the onset of melting was observed and $T_{m,2}$ is the temperature at which the samples were noted to be in a complete liquid state.

Particular attention was given to avoid air gaps and to ensure equal quantity of salt mixtures inside the tubes. The small tube size assured a favourable heat transfer to the salt mixtures due to the low thermal inertia. However, on occasions, this hindered the homogeneity of the sample, as some single salt clusters were observed separating from the salt mixture during testing.

Firstly, a validation of the experimental procedure was performed, with the aim of reproducing the melting points of the starting-point commercial salt mixtures reported in the literature. Table IV presents the experimental data for validation using the 5 chosen starting-point commercial salt mixtures. The HITEC, LiK and LiNaK results were reproduced within 1-3˚C of the published values. However, a greater discrepancy was noted for the quaternary mixtures, with errors of 11-19˚C. This may be attributed to a three-fold challenge. Firstly, the precision required for the individual components (e.g. mass fraction of 14.2 for $NaNO_3$ in Quaternary). Secondly, the complexity associated with an increased number of individual mixture components. Thirdly, due to the individual components purity being 99% (rather than 99.99%) to ensure an economical molten salt TES and HTF solution.

Table IV. Experimental validation of melting point of the 5 chosen starting-point commercial salt mixtures using published literature.

Molten Salt Name	Literature [T_m ℃]	Experiment [T_m ℃]	[ΔT ℃]
HITEC	142	143	1
LiK	133	132	-1
LiNaK	120	123	3
Quaternary	99	118	-19
CaLiNaK	72	86	-11

Following the validation of the experimental procedure, tests were conducted on the two classifications of alternative salt mixtures. Fig.5 (a-c) presents the field of view images during the successful testing of an alternative composition of LiNaK constituents. However, in limited number of cases, testing was discontinued as complete melting was not observed below 200˚C. Thus, making the salt mixture unsuitable for the considered CSP and LAES applications. Fig.5 (d-f) presents such an unsuccessful testing example of an alternative composition of HITEC constituents.

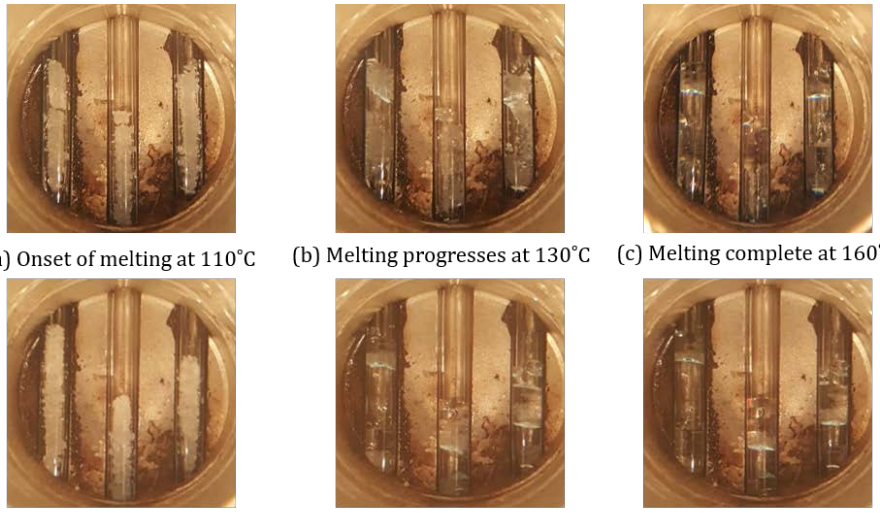

(a) Onset of melting at 110˚C (b) Melting progresses at 130˚C (c) Melting complete at 160˚C

(d) Onset of melting at 110˚C (e) Melting progresses at 172˚C (f) Melting incomplete at 192˚C

Fig.5. Example of melting temperature field of view images in case of a successful test (a-c, LiNaK-5) and in a discontinued test (d-f, HITEC-8).

Table V details the composition of the 13 alternative new molten salt mixtures, their average volumetric heat capacities between 100-400˚C and the experimentally identified melting point. Also included are the, variation in volumetric heat capacity and melting temperature compared to the respective starting-point commercial molten salts. It can be noted that, most of the alternative salt mixtures with different compositions and higher values of volumetric heat capacities (10-24%) also resulted in a noticeable increase in the melting point temperature (62-107˚C) with respect to the starting-point mixtures. Whereas, the alternative salt mixtures with similar compositions resulted in a compromised solution, with small increases in volumetric heat capacities (1-15%) and melting point temperature (17-46˚C) with respect to the starting-point mixtures. More importantly, two alternative mixtures (CaLiNaK 11 and 4), which were associated with higher volumetric heat capacity improvements (15-19%), were identified to give a preferred trade-off, resulting in only moderate increases in melting point temperature (20-30˚C) with respect to the starting-point mixture.

Table V. Summary of the 13 alternative new molten salt mixtures, including mass composition, change in volumetric heat capacity and change in experimental melting point (- means that complete melting was not observed below 200˚C)

Salt Name	ID	Composition	$c_v \left[\frac{MJ}{m^3K}\right]$	$\Delta c_v \left[\frac{MJ}{m^3K}\right]$	T_m [°C]	ΔT[°C]	σ
HITEC	5	Different	3.32	10%	-	-	-
	8	Different	3.52	17%	-	-	-
	2	Similar	3.10	3%	162	20	5.7
	4	Similar	3.31	10%	172	30	3.3
LiK	3	Different	3.27	18%	-	-	-
LiNaK	5	Different	3.26	13%	-	-	-
	2	Similar	3.04	5%	137	17	2.3
Quaternary	25	Different	3.57	20%	175	76	2.3
	11	Similar	2.99	1%	145	46	2.5
	2	Similar	3.24	9%	160	61	3.1
CaLiNaK	4	Different	3.74	19%	95	20	7.9
	17	Different	3.88	24%	-	-	-
	11	Similar	3.60	15%	105	30	7.2

Fig.6 presents the trade-off maps to compare the volumetric heat capacity and the melting point for all the relevant experimentally tested mixtures, concerning three different temperature ranges, namely < 100°C, 100-150°C, and < 200°C. Points are labelled with the corresponding ID number reported in Table V, or 1 when referring to the starting-point commercial salt mixtures. The three graphs of Fig.6 shows how the present work has introduced in all the different temperature ranges, at least one appealing alternative mixture composition which, in most cases, provides a comparable melting point but higher volumetric heat capacity.

In Fig.6a, together with the starting-point mixtures of Quaternary and CaLiNaK, alternative CaLiNaK 4 has similar melting point but significantly higher volumetric heat capacity. In Fig.6b, the alternative CaLiNaK 11 is attractive due to its lower melting point and noticeably higher volumetric heat capacity. Fig.6c consists of

alternative mixtures only. However, Quaternary 25 provides the greatest increase in the volumetric heat capacity compared to the starting-point mixture.

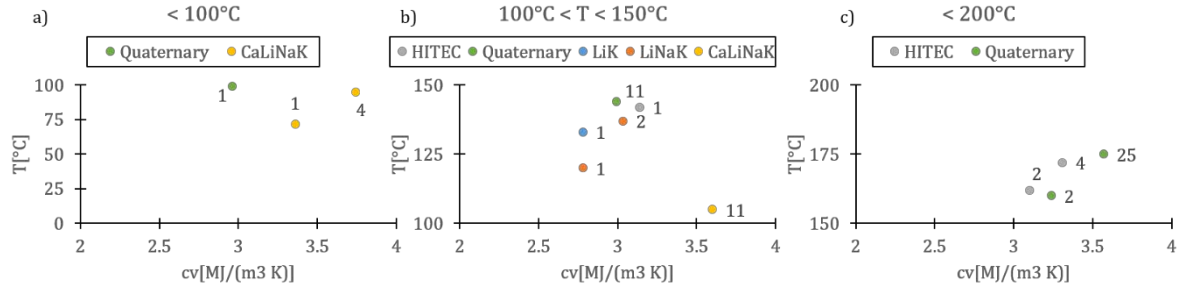

Fig.6. Experimental melting point temperature vs. volumetric heat capacity map, for the chosen 5 starting-point commercial salt mixtures and the alternative new salt mixtures.

These three trade-off maps have identify temperature tailored 3 new molten salts for application such as CSP and LAES. Namely CaLiNaK 4 and 11, and Quaternary 25, which offer low melting temperatures and beneficial thermo-physical properties. Table VI details the composition of these 3 new potential salt mixtures as future candidates for use as both thermal energy storage and heat transfer fluid.

Table VI. Composition of 3 new potential molten salt mixtures to act as both thermal energy storage and heat transfer fluid.

Salt ID	Composition (wt%)
Quaternary-25	25NaNO3-5KNO3-5LiNO3-65NaNO2
CaLiNaK-4	45NaNO3-25KNO3-5LiNO3-25Ca(NO3)2
CaLiNaK-11	25NaNO3-45KNO3-5LiNO3-25NaNO2

4. Conclusions

This work was focused on the identification and evaluation of low temperature molten salt mixtures as the feasible common medium for both the thermal store and the heat transfer fluid for sustainable energy systems. The parameters for evaluation were the melting point temperature and the volumetric heat capacity. Two classifications of mixtures were considered: similar compositions and noticeably different compositions to the starting-point commercial salts. The significant findings of the present work are as follows:

1. Nitrate-based salt mixtures were identified for detailed investigation as they offered higher volumetric heat capacities (2.8-3.1 vs. 1.7-2.1 MJ/m^{3}K) and comparable average melting point temperatures (113 vs. 108˚C) compared to the chloride-based salt mixtures.
2. The considered experimental procedure provided a low variation in melting point temperature against the published literature. For example, HITEC, LiK and LiNaK results were reproduced within 1-3˚C.
3. Experimental investigations identified the melting point of 8 alternative new molten salt mixtures in the range of 95-175˚C (Table V).
4. Melting temperature and volumetric heat capacity trade-off maps were produced using the starting-point commercial molten salts and the alternative new salt mixtures for different temperature ranges (< 100 ˚C, 100-150˚C, < 200 ˚C). These maps offer a guide in the selection of suitable molten salts, depending on the temperature requirements, to improve the overall system efficiency and feasibility.
5. Three alternative new molten salt mixtures, which included two from the CaLiNaK family (CaLiNaK 11 and 4), were identified as preferred candidates due to higher improvements in volumetric heat capacity (15-19%) and only moderate increases in melting point temperature (20-30˚C) compared to CaLiNaK.

Acknowledgement

This work was funded by INNOVATE UK “Development of High Grade Heat Storage for integration with Liquid Air Energy Storage” (Ref 133465) project. The Authors’ would like to acknowledge the support of the industrial partner Highview Power Storage Ltd. (Johnny Cochrane and Edward Scrase) and the School of Pharmacy and Biomolecular Sciences (Dr. Petra Kristova).

References

1. B. Ameel, C. T’Joen, K. De Kerpel, P. De Jaeger, H. Huisseune, M. Van Belleghem, and M. De Paepe, Appl. Therm. Eng. **52**, 130 (2013).
2. F. Crotogino, G. S. Schneider, and D. J. Evans, Proc. Inst. Mech. Eng. Part A J. Power Energy **232**, 100 (2018).
3. L. Coco-enriquez, J. Muñoz, and J. María, J. Polytech. **18**, 219 (2015).

4. E. González-Roubaud, D. Pérez-Osorio, and C. Prieto, Renew. Sustain. Energy Rev. **80**, 133 (2017).
5. R. K. M. Aldulaimi and M. S. Söylemez, Int. J. Renew. Energy Dev. **5**, 151 (2016).
6. G. Karaca, E. C. Dolgun, M. Koşan, and M. Aktaş, J. Energy Syst. **3**, 86 (2019).
7. International Renewable Energy Agency (IRENA), *Renewable Power Generation Costs in 2012: An Overview* (2013).
8. H. Peng, X. Shan, Y. Yang, and X. Ling, Appl. Energy **211**, 126 (2018).
9. R. Morgan, S. Nelmes, E. Gibson, and G. Brett, Appl. Energy **137**, 845 (2015).
10. L. Chen, T. Zheng, S. Mei, X. Xue, B. Liu, and Q. Lu, J. Mod. Power Syst. Clean Energy **4**, 529 (2016).
11. X. She, X. Peng, B. Nie, G. Leng, X. Zhang, L. Weng, L. Tong, L. Zheng, L. Wang, and Y. Ding, Appl. Energy **206**, 1632 (2017).
12. R. Serrano-ópez, J. Fradera, and S. Cuesta-López, Chem. Eng. Process. - Process Intensif. **73**, 87 (2013).
13. P. Gimenez and S. Fereres, Energy Procedia **69**, 654 (2015).
14. M. Medrano, A. Gil, I. Martorell, X. Potau, and L. F. Cabeza, Renew. Sustain. Energy Rev. **14**, 56 (2010).
15. A. Bonk, S. Sau, N. Uranga, M. Hernaiz, and T. Bauer, Prog. Energy Combust. Sci. **67**, 1339 (2018).
16. Y. T. Wu, Y. Li, N. Ren, R. P. Zhi, and C. F. Ma, Sol. Energy Mater. Sol. Cells **176**, 181 (2018).
17. G. Zheng and K. Sridharan, Jom **70**, 1535 (2018).
18. T. Bauer, N. Breidenbach, and M. Eck, in *World Renew. Energy Forum 2012* (2012), pp. 1–8.
19. K. Vignarooban, X. Xu, A. Arvay, K. Hsu, and A. M. Kannan, Appl. Energy **146**, 383 (2015).
20. A. Gil, M. Medrano, I. Martorell, A. Lázaro, P. Dolado, B. Zalba, and L. F. Cabeza, Renew. Sustain. Energy Rev. **14**, 31 (2010).
21. C.-J. Li, P. Li, K. Wang, and E. Emir Molina, AIMS Energy **2**, 133 (2014).
22. V. M. B. Nunes, C. S. Queirós, M. J. V. Lourenço, F. J. V. Santos, and C. A. Nieto de Castro, Appl. Energy **183**, 603 (2016).
23. M. M. Kenisarin, Renew. Sustain. Energy Rev. **14**, 955 (2010).
24. R. H. Perry, B. E. Poling, G. H. Thomson, D. G. Friend, R. L. Rowley, and W. Vi. Wilding, *Perry's Chemical Engineers' Handbook, Physical and Chemical Data* (2008).
25. L. Kourkova, R. Svoboda, G. Sadovska, V. Podzemna, and A. Kohutova, Thermochim. Acta **491**, 80 (2009).
26. J. McMurry, Belmont, CA Brooks Cole/Cengage Learn. 2012. (2012).